



PRACTICAL LINEAR AND NONLINEAR MODELS OF REINFORCED CONCRETE BEAM-COLUMN JOINTS IN EXISTING STRUCTURES

Anna Birely¹, Laura Lowes² and Dawn Lehman²

ABSTRACT

Beam-column joint damage can significantly impact the performance of reinforced concrete moment frames subject to earthquake loading, and, in extreme cases, can contribute to frame collapse. To assess the seismic performance of existing concrete frames, engineers require models that can accurately predict the behavior of joints for a wide range of designs and that are easily implemented in commercial software. In this study, a database of 45 planar interior beam-column joints is used to evaluate two types of joint models. First, models acceptable for linear analyses are considered. The rigid offset models recommended in the ASCE/SEI Standard 41-06 are evaluated, and a modified approach to determining the rigid offset length is proposed to provide improved prediction of the displacement at which beams yield. Second, a model is developed to support nonlinear modeling of frames and enable simulation of progressive joint stiffness and strength loss. A number of nonlinear joint models can be found in the literature, but few are easily implemented in commercial design/analysis software or verified for a range of joint designs. In this study, a simple nonlinear model is proposed in which lumped-plasticity beam elements are modified to account for joint flexibility and potential strength loss. Specifically, the beam-element plastic hinge is assumed to represent two nonlinear hinges in series. The first hinge represents the flexural response of the beam, and the second represents the nonlinear response of the joint. The beam flexural hinge is defined by the traditional moment-curvature response of the beam section and a newly developed rotation limit at which strength loss is predicted. The joint hinge is bilinear, with stiffnesses calibrated to accurately predict measured response, and includes a rotation limit at which strength loss initiates due to joint failure. The proposed model accurately predicts the load-displacement response of frame sub-assemblages including accurately predicting the mechanism that determines response: beam flexure or joint failure.

¹Graduate Research Assistant, Dept. of Civil & Environmental Engineering, University of Washington, Seattle, WA

²Associate Professor, Dept. of Civil & Environmental Engineering, University of Washington, Seattle, WA

Introduction

Beam-column joints in RC moment frames can contribute significantly to frame flexibility and strength loss during an earthquake. Thus, practical models are required to enable engineers to simulate joint response and its impact on overall frame response. A wide range of models for RC beam-column joints are found in the literature. The simplest, found in the ASCE/SEI Standard 41-06 (2006), includes rigid offsets at the ends of beam and column elements that are varied in length to simulate the flexibility of the joint region. Other recent models include those presented by Anderson et. al. (2007) in which empirically calibrated nonlinear rotational springs connect beam and column centerline elements. Nonlinear models in which finite-volume joint macro-elements have been proposed (Mitra and Lowes 2007, Shin and Lafave 2004, and Lowes et al. 2003) to account for flexibility due to slip of beam longitudinal reinforcement and shear action within the joint core. Despite the variety of alternatives available for modeling beam-column joints, few meet the requirements necessary for widespread use in practice: 1) compatibility with commonly employed commercial software packages, 2) support for rapid model building, 3) computational efficiency and robustness, and 4) acceptable accuracy over a range of design configurations.

Two practical methods for modeling joint response are discussed in this paper. First, rigid offset models, which are appropriate for elastic analysis, are considered. The model presented included in the ASCE/SEI Standard 41-06 is evaluated. Recommendations are made to improve the prediction of initial joint stiffness using rigid offset length determined as a function of joint design parameters. Second, a nonlinear model is proposed that modifies lumped plasticity beam elements to account for joint flexibility. Both linear and nonlinear models are evaluated using an extensive experimental data set of joint tests with a wide range of design parameters representing both modern and older detailing.

Experimental Data Set

For evaluation of existing models and calibration of proposed models, a data set of planar interior beam-column joint sub-assemblages was developed from that presented by Mitra and Lowes (2007). The data set comprises sub-assemblages without i) slabs or transverse beams, ii) failure modes of beam shear, column flexure or column splice failure, and iii) smooth reinforcing bars. All specimens were subject to reversed cyclic lateral loading, to represent earthquake loading. Test specimens were evaluated to determine if joint designs satisfied the seismic design criteria of the ACI Building Code (2008) for Special Moment Frames, and thus whether or not joint damage could be expected to limit subassemblage ductility under seismic loading. ACI compliance was determined on the basis of joints meeting the requirements for 1) concrete compressive strength and reinforcement yield strength, 2) the ratio of the sum of the column flexural strengths to the sum of the beam flexural strengths 3) presence of lap splices or termination of beam reinforcement in the joint 4) ratio of column height to beam longitudinal reinforcement diameter 5) amount and spacing of joint transverse reinforcement and 6) nominal joint shear stress demand (Eq. 1). Eleven joints were found to be ACI Compliant and 34 were found to be ACI Non-Compliant, having failed to meet at least one of the above requirements.

Evaluation of the experimental data indicated that a number of design parameters affect the seismic performance of joints; however, shear and beam-bar bond stress demand were found

to be the most critical and were used to refine the joint models. Shear stress demand, τ_{design}^{norm} was computed using the approach recommended by ACI Committee 352:

$$\tau_{design}^{norm} = \frac{1}{\sqrt{f'_c h_c b_j}} \alpha (f_y (A_s^{top} + A_s^{bot}) - V_c) \quad (1)$$

where h_c is the column depth, b_j is the out-of-plane dimension of the joint, f_c is the concrete compressive strength, f_y is the measured yield strength of the beam longitudinal reinforcing steel, A_s^{top} and A_s^{bot} are the area of the steel in the top and bottom of the beam, respectively, and α is defined as 1.25/1.11, rather than the 1.25 recommended by Com. 352, to account for the fact that f_y is the measured rather than nominal yield strength of the reinforcing steel. For the data set, shear stress demands had a mean value of 19.4 and a standard deviation of 9.8. The bond index, μ , was defined as the normalized maximum beam-bar bond stress in the joint assuming the bars yield:

$$\mu = \frac{f_y d_b}{2 h_c \sqrt{f'_c}} \quad (2)$$

where d_b is the maximum diameter of the beam longitudinal reinforcement and all other variables are as defined in Eq. 1. For the data set, the mean bond index was 25.3, with a standard deviation of 11.0.

Linear Models

Rigid offset models are easily implemented in commercial structural analysis software and, thus, are a practical tool for engineers to use to simulate joint flexibility in linear elastic analysis of RC frames. In a basic line-element model of a frame, the flexural, shear and torsional stiffness of frame elements are determined from frame member dimensions and material properties. Often, *effective* stiffness are employed for frame elements; these effective stiffness represent a reduction from the gross section stiffnesses that are computed using member gross section dimensions and elastic material properties and are intended to simulate the impact of cracking under service level loading on member stiffness. In the typical line-element model, beams and columns intersect at a node located at the center of the “joint”. Often, the joint region is assumed to be rigid, and this rigidity is simulated by introducing rigid offsets at the ends of beams and columns within the joint volume. The length of these rigid offsets can be adjusted to enable simulation of the joint flexibility observed in the laboratory. In this study, existing recommendations for offset lengths were evaluated using the previously discussed experimental data set. Additionally, new offset length recommendations were made to improve prediction of frame response.

First, simple centerline models were created of the 45 sub-assemblages in the data set. In these models, rigid offsets were not included at member ends within the joint (Fig. 1a) and beam and column effective stiffnesses were defined using the recommendations of ASCE/SEI Standard 41-06. Models were loaded with the appropriate column axial load and with a column shear corresponding to first yield of the beams (or maximum load if beams did not yield) in flexure. For each sub-assemblage, i , the analytical displacement, $(\Delta_{sim}^{yield})^i$, at the yield load was

compared with the experimental displacement, $(\Delta_{exp}^{yield})^i$, at the yield load. The error in the predicted displacement was computed as the difference between the experimental and simulated displacements, normalized by the experimental displacement:

$$\varepsilon_i = \frac{(\Delta_{exp}^{yield})^i - (\Delta_{sim}^{yield})^i}{(\Delta_{exp}^{yield})^i} \quad (3)$$

For a number of joint subassemblages, the centerline model (without rigid offsets within the joint region) was stiffer than the experimental sub-assemblage. For these subassemblages, the introduction of beam and/or column rigid offsets within the joint increases the error in predicted displacement, and rigid offset lengths cannot be found that reduce the error in predicted yield displacement. Thus, a reduced dataset of 26 specimens that excluded these sub-assemblages was formed for model calibration purposes.

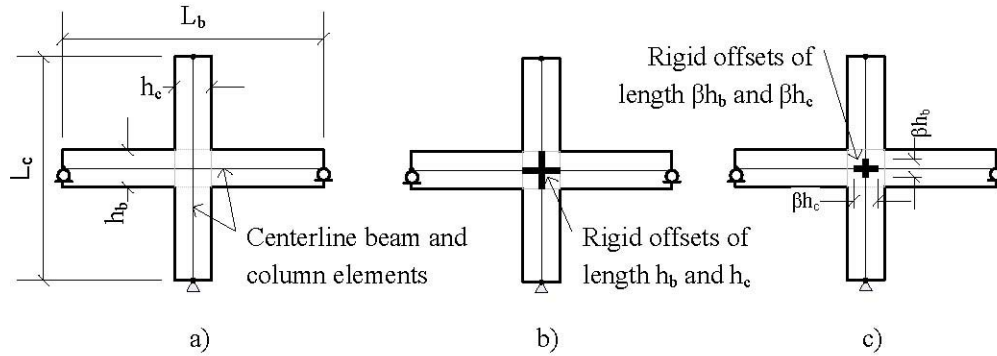


Figure 1. Centerline models of sub-assemblages with a) no offsets, b) full length offsets, and c) offsets using proposed β factor applied.

Next, the recommendations in ASCE/SEI Standard 41-06 and its predecessor, FEMA 356, were evaluated. FEMA 356 recommends offset lengths equal to the full joint dimensions (Fig. 1b) and effective bending stiffness values for frame elements of $0.5-0.7EI_g$. ASCE/SEI Standard 41-06 recommends lower effective stiffness values for frame members of $0.3-0.7EI_g$ and rigid offset lengths i) equal to full column depths for beams only for the case of $\Sigma M_{nc}/\Sigma M_{nb} < 0.8$, ii) the full beam depth for columns only for the case of $\Sigma M_{nc}/\Sigma M_{nb} > 1.2$, or iii) half the joint dimensions in the beams and columns for the case of $0.8 < \Sigma M_{nc}/\Sigma M_{nb} < 1.2$, where M_n is the nominal flexural strength of the beam or column and moments are summed at the center of the joint.

Finally, the reduced dataset was used to develop rigid offset length recommendations that improved prediction of secant stiffness to yield. Effective stiffnesses values from ASCE/SEI Standard 41-06 were used for the frame members, and rigid offsets were included at the ends of both the beams and columns. Rigid offset lengths were defined as a percentage, β , of the joint dimensions (Fig. 1c). β values were found for i) all joints in the reduced data set, ii) ACI compliant joints in the reduced data set, and iii) ACI non-compliant joints in the reduced data set. The factor β was found using two methods. First, a single value was found by minimizing the

sum of the square of the displacement errors, ϵ_i (Eq. 3), of the specimens in the reduced data set. This *optimal* β value was rounded to a *proposed* single significant digit to facilitate application in practice. These β values are presented in Table 1 and show that frames with ACI compliant joint designs are most accurately modeled with stiffer joints than frames with ACI non-compliant joints. Next, relationships were sought between joint design parameters and the optimal offset length for individual sub-assemblages, where the optimal offset length for specimen i minimizes ϵ_i . Normalized shear stress demand, τ (Eq. 1), and bond demand, μ (Eq. 2), were found to correlate with the offset length needed to accurately predict experimental initial stiffness, and a *functional* offset length model was developed. The form of this functional offset model is presented in Table 1.

Table 1. Rigid offset lengths calibrated with reduced data set

Calibration Method	All	ACI Compliant	ACI Non-Compliant
Optimal Exact	$\beta = 0.44$	$\beta = 0.62$	$\beta = 0.39$
Optimal Proposed	$\beta = 0.4$	$\beta = 0.6$	$\beta = 0.4$
Optimal Functional	$\beta = 0.92 - 0.02\mu$	$\beta = 1.87 - 0.04\tau - 0.05\mu$	$\beta = 0.81 - 0.02\mu$

Tables 2 presents the average and standard deviation of the error given by Eq. 3 for the reduced data set and all of the models considered in the study. Specifically, error measures are provided for the modeling recommendations in FEMA 356, in ASCE/SEI Standard 41-06, and developed as part of this study. Additionally, error data are provided for models employing the ASCE/SEI Standard 41-06 beam and column effective stiffnesses for the case of no offsets, $\beta = 0.0$, and for the case of a fully rigid joint, $\beta = 1.0$. Error measures are included for all joints in the reduced dataset as well as for the ACI compliant and ACI non-compliant datasets.

Table 2. Error evaluation for rigid offset models: reduced data set

Model	All Specimens		ACI Compliant Specimens		ACI Non-Compliant Specimens	
	Avg.	Std. Dev.	Avg.	Std. Dev.	Avg.	Std. Dev.
FEMA 356 ¹	0.53	0.07	0.50	0.08	0.54	0.07
Fully rigid joint ($\beta=1$) ²	0.24	0.12	0.17	0.14	0.25	0.12
SEI/ASCE 41-06 ²	0.04	0.14	-0.04	0.17	0.06	0.13
Optimal - Exact ²	0.02	0.15	0.02	0.16	0.01	0.14
Optimal - Proposed ²	0.02	0.15	0.01	0.17	0.02	0.14
Optimal - Functional ²	0.001	0.12	0.002	0.05	0.004	0.12
Centerline ($\beta=0$) ²	-0.19	0.17	-0.28	0.21	-0.16	0.16

Notes: 1. Beam and column effective stiffness defined per FEMA 356. 2. Beam and column effective stiffness defined per ASCE/SEI Standard 41-06.

The data in Table 2 show that application of the FEMA 356 recommendations resulted in a significant over-prediction of the stiffness of the frame subassemblages and that application of the ASCE/SEI Standard 41-06 recommendations significantly improved the prediction of yield displacement. The error data for the case of fully rigid joints ($\beta = 1$) with ASCE/SEI Standard 41-06 member effective stiffnesses, shows that improved simulation of member stiffness

contributed significantly to overall improvement in displacement prediction. The data in Table 2 show also that the rigid offset length recommendations developed as part of this study provide a modest improvement over the current ASCE/SEI Standard 41-06 recommendations. If only compliance with the ACI Code requirements for joint design is considered, the average error in yield displacement is reduced at a minimum from 4% with the ASCE/SEI Standard 41-06 model to 2% with the proposed model and at most from 6% to 1% for non-compliant joints. Using the proposed functional models, the average error in yield displacement is reduced at a minimum from 4% with the ASCE/SEI Standard 41-06 model to 0.2% with the proposed model and at maximum from 6% to 0.4% for non-compliant joints.

Nonlinear Model

Rigid offset models are simple and can provide reasonable prediction of initial stiffness. However, they lack the ability to capture the changes in joint stiffness associated with beam yielding and strength loss due to joint damage, behaviors exhibited in joints during seismic loading. To facilitate nonlinear modeling of joint response using commercial software, a model was developed in which the moment-rotation response of the plastic hinge in a lumped-plasticity beam element was modified to account for additional flexibility and potential strength loss resulting from joint damage.

Fig. 2 shows a model of a frame sub-assembly employing lumped plasticity beam elements. Columns and beams, outside of the hinge, are assigned effective stiffness values according to the recommendations of ASCE/SEI Standard 41-06. Rigid offsets define the physical joint region as rigid ($\beta=1.0$). The lumped plasticity beam elements have a plastic hinge located at the face of the joint. Typically, hinge response would be defined using the results of a moment-curvature analysis of the beam cross-section and a plastic-hinge length (typically a length of one-half the beam depth is used). This model does not explicitly account for the nonlinear behavior of the joint. Thus, a modified model was developed, in which the beam plastic hinge is modified to include two rotational springs in series. One spring represents the nonlinear flexural behavior of the beam; the other represents the nonlinear behavior of the joint. Rotational limits allow the model to account for loss of lateral load carrying capacity. Fig. 3 illustrates moment-rotation responses of the individual and combined springs.

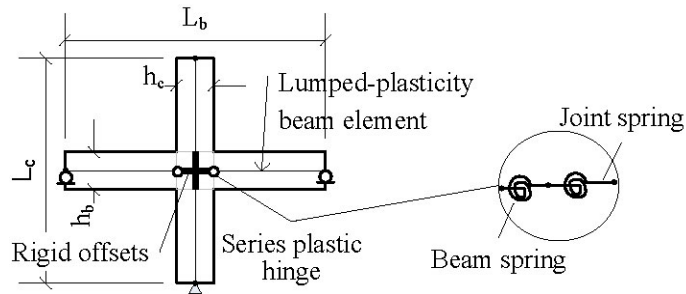


Figure 2. Nonlinear model of sub-assembly using modified lumped plasticity beam elements

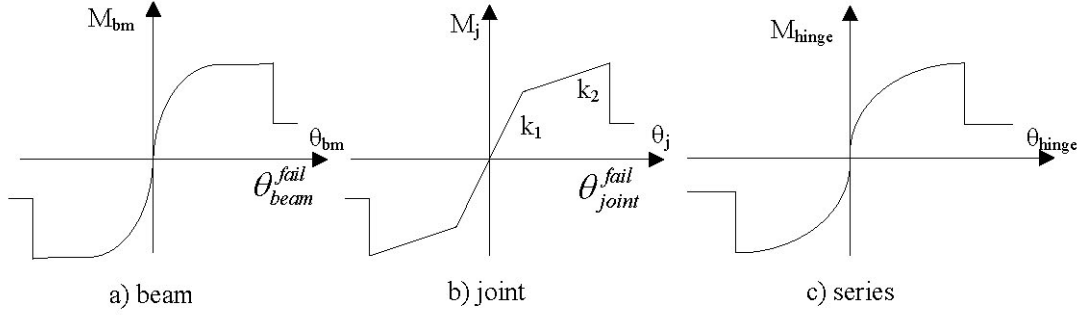


Figure 3. Moment-rotation curve for a) beam spring, b) joint spring, and c) the combined beam and joint springs making the series plastic hinge.

To develop the joint moment-rotation model, it is assumed that a joint responds primarily in shear and the shear stress-strain behavior of the joint is transformed to a moment-rotation relationship by imposing compatibility and equilibrium requirements. Using this approach, the moment-rotation stiffness, k , of the joint spring may be written:

$$k = \frac{M}{\theta} = \frac{\chi_{\tau} \tau}{\chi_{\gamma} \gamma} \quad (4)$$

where frame geometry determines the modifiers:

$$\chi_{\tau} = A_j \left(1 - \frac{h_c}{L_d} \right) jd / 2 \left(1 - \frac{jd}{L_c} - \frac{h_c}{L_b} \right) \quad (5)$$

$$\chi_{\gamma} = 1 - \frac{h_b}{L_c (1 - h_c / L_b)} \quad (6)$$

and h_b and h_c are, respectively, the depth of the beam and column, L_b is the column-to-column centerline length of beam, L_c is the beam-to-beam centerline height of the column, A_j is the cross-sectional area of the joint, and jd is the lever arm of the beam moment. Introducing the concrete shear modulus:

$$G = \frac{\tau}{\gamma} \quad (7)$$

the joint stiffness in the proposed model may be defined, for each segment, i , of a multi-linear response model:

$$k_i = \alpha_i \frac{\chi_{\tau}}{\chi_{\gamma}} G \quad (8)$$

where α_i is a calibrated modification factor .

The joint spring was placed in the plastic hinge in series with a moment-rotation spring representing the beam response, developed from a moment-curvature analysis of the beam (performed in OpenSees (McKenna, et. al., 2007)) and an assumed plastic hinge length of one-half the depth of the beam. Together, these springs combined to produce a modified plastic-hinge model that accounts for joint flexibility. To represent strength loss, rotational limits were placed on the beam and joint springs. These limits were calibrated using experimental data.

Model Calibration

The initial joint stiffness was calibrated by optimizing the secant stiffness of the plastic hinge at the column shear corresponding to initial yielding of the beams, where the joint initial stiffness is defined by the calibrated stiffness parameter $\alpha_1 = 0.14$.

The post-yield stiffness of the joint spring was established using data for joints in which both beam on both the right and left sides of the joint yielded. This was done to ensure accurate simulation of post-yield response, specifically to enable calibration of rotation limits (for loss of lateral strength capacity) in the joint shear spring and beam springs to achieve simulation of displacement ductility. The resulting stiffness parameter was $\alpha_2 = 0.038$.

To calibrate rotation limits for the joint and beam hinges, a method for classifying and predicting the response mode of each joint test specimen was needed. Data for specimens classified as “brittle” were used to calibrate the rotation limit for the joint hinge; while, data for specimens classified as “ductile” were used to calibrate the rotation limit for the beam hinge. The joints were classified according to the level of displacement ductility (μ_Δ) achieved at 10% loss in the maximum strength. Displacement ductility of unity (1.0) was defined at the column shear associated with theoretical beam yielding. Joints were identified as "Brittle" if they did not reach this column shear. For those joints that reached or exceeded this yield force, those with a displacement ductility of at least 4.0 were identified as "Ductile". Joints between these limits were identified as "Limited Ductility". Eighteen joints were classified as "Brittle", twenty as "Ductile", and seven as "Limited Ductility".

The rotational limit for the beam hinge was determined by finding the curvature minimizing the average drift error at strength loss of ductile joints, where the curvature and rotation are related by:

$$\theta_{bm}^{fail} = l_p \phi_{bm}^{fail} = l_p 0.0056 \quad (9)$$

where l_p is the plastic hinge length defined equal to half the beam depth for the current study.

The joint rotational limit was calibrated by minimizing the average drift error of brittle joints at strength loss, and was defined as a function of joint shear strains and system geometry:

$$\theta_{joint}^{fail} = \chi_\gamma \gamma_{joint}^{fail} = \chi_\gamma 0.0069 \quad (10)$$

where χ_γ is as defined in Eq. 6.

Model Validation

To evaluate the proposed nonlinear model, pushover analyses were performed on models of the joint sub-assemblages. The analytical load-drift envelopes were compared with the experimental envelopes at key points in the load-drift histories: 1st yield (any beam yields), 2nd yield (both beams have yielded), peak strength, and 10% loss of lateral load carrying capacity. The error at these points was calculated as the difference between experimental and analytical values, normalized by the experimental value. Table 3 provides the average error in load and drift as well as the standard deviation of this error at the identified key points of the response history. Fig. 4 shows the best worst simulation of experimental response for brittle and ductile joints.

Table 3. Error of proposed nonlinear joint model at key points of the response history

Data Sub-sets	Error	1 st Yield ¹	2 nd Yield ¹	Peak Strength		10% Strength Loss	
		Disp	Disp	Disp	Load	Disp	Load
All ²	Average	6%	14%	-32%	5%	26%	6%
	Stand. Dev.	23%	25%	78%	10%	34%	11%
Ductile	Average	8%	18%	-61%	8%	8%	2%
	Stand. Dev.	25%	25%	90%	7%	36%	9%
Limited Ductility	Average	-4%	-2%	-20%	12%	46%	9%
	Stand. Dev.	24%	25%	84%	8%	41%	13%
Brittle	Average	-	-	-4%	-1%	-	-
	Stand. Dev.	-	-	53%	10%	-	-

¹For 1st and 2nd yield, excludes joints not the corresponding yield force

The data in Table 3 and Fig. 4 show that the model enables accurate simulation of response. At the column shear corresponding to first yield, the data in Table 3 show that displacement was predicted very well, indicating the ability of the proposed model to adequately capture the initial stiffness of the assemblages. Brittle joints had a low error for displacement and force at the peak strength. Although there was significant scatter in this error for the displacement, the peak force had a low standard deviation, indicating the accuracy of the model in predicting the strength capacity of the brittle joints. For ductile and limited ductility joints, the error in peak strength and the standard deviation of this error are low (less than 13%). For ductile and limited ductility joints, the average error in the predicted displacement at peak strength and the standard deviation on this error are large; however, this is a function of the relatively small stiffness of the system in the vicinity of peak strength and, thus, provides limited information on model accuracy, as the moment capacity of the beam, determined through moment-curvature analysis, controlled this aspect of the model.

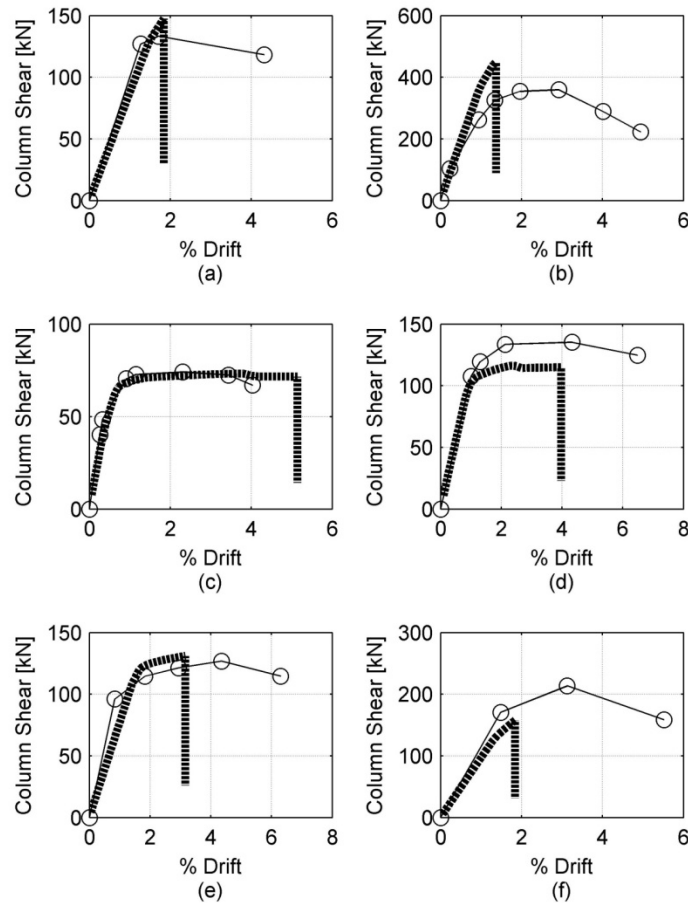


Figure 4. Envelopes for (a) best brittle prediction, MJ3, (b) worst brittle prediction, PEER22, (b) best ductile prediction, PR3, (d) worst ductile prediction, HC, (e) best limited ductility prediction, PM1 and (f) worst limited ductility prediction, MJ12.

The proposed model may be evaluated also on the basis of the accuracy with which the failure mechanism is simulated. For all “Ductile” joints, strength loss was simulated to occur when the beam rotation limit was reached. For all “Brittle” joints, strength loss was simulated to occur when the joint spring rotation limit was reached. Thus, the model accurately predicted the failure mechanism for these joints. Of the seven "Limited Ductility" joints, six exhibited strength loss when the joint rotation limit was reached, and thus exhibited brittle failure in the simulation.

Conclusions

The rigid offset approach for modeling beam-column joint behavior, recommended by ASCE/SEI Standard 41-06 for evaluation of existing structures and easily implemented in commercial software, improved the prediction of experimental joint stiffness prior to beam yielding when compared to the recommendations of FEMA 356. Proposed recommendations were developed using an extensive data set of beam-column joint sub assemblages, where offset length was determined based on joint shear stress demand and bond demand of beam

longitudinal reinforcement passing through the joint. Using this method, the error in prediction of the initial joint stiffness was reduced approximately 40% over the ASCE/SEI Standard 41-06.

To provide an easily implemented model capable of capturing post-yield behavior of joints, including loss of lateral load carrying capacity, a nonlinear model was developed that modified lumped-plasticity beam elements to account for joint behavior. The joint was modeled using bilinear moment-rotation springs, with stiffness defined as a function of sub-assembly geometry and the concrete shear modulus. Loss of lateral load carrying capacity was accounted for through rotational limits in the plastic hinge. Separate limits for the beam and joint behavior within the plastic hinge allowed the model to account for both brittle and ductile failure modes independent of prior knowledge of the failure mode.

Acknowledgement

Support of this work was provided primarily by the Earthquake Engineering Research Centers Program of the National Science Foundation, under award number EEC-9701568 through the Pacific Earthquake Engineering Research Center (PEER). Any opinions, findings, and conclusions or recommendations expressed in this material are those of the authors and do not necessarily reflect those of the National Science Foundation.

References

- ACI Committee 318, 2008. *Building code requirements for structural concrete (ACI 318-08) and Commentary (ACI 318R-08)*, American Concrete Institute, Farmington Hills, Michigan
- ACI-ASCE Joint Committee 352, 2005. *Recommendations for design of beam-column connections in monolithic reinforced concrete structures*, American Concrete Institute, Farmington Hills, Michigan.
- Anderson, M., Lehman, D., and Stanton, J, 2008. A cyclic shear stress-strain model for joints without transverse reinforcement, *Engineering Structures*, 30(4), pp. 941-954.
- ASCE, 2000. *Pre-standard and Commentary for the Seismic Rehabilitation of Buildings (FEMA-356)*, American Society of Civil Engineers prepared for the Federal Emergency Management Agency, Reston, Virginia.
- ASCE, 2007. *Seismic Rehabilitation of Existing Buildings (ASCE/SEI 41-06)*. American Society of Civil Engineers.
- Lowes, L.N., Mitra, N., and Altoontash, A., 2004. A beam-column joint model for simulating the earthquake response of reinforced concrete frames, Pacific Earthquake Engineering Research Center, Berkeley, California.
- McKenna, F., Fenves, G.L., et al, 2007. *Open Systems for Earthquake Engineering Version 1.7.3*, <http://opensees.berkeley.edu>.
- Mitra, N., and Lowes, L.N., 2007. Evaluation, calibration, and verification of a reinforced concrete beam-column joint, *Journal of Structural Engineering*, 133(1), pp. 105.
- Shin, M., and Lafave, J.M., 2004. Modeling of cyclic joint shear deformation contributions in RC beam-column connections to overall frame behavior, *Structural Engineering and Mechanics*, 18(5), pp. 645-669.